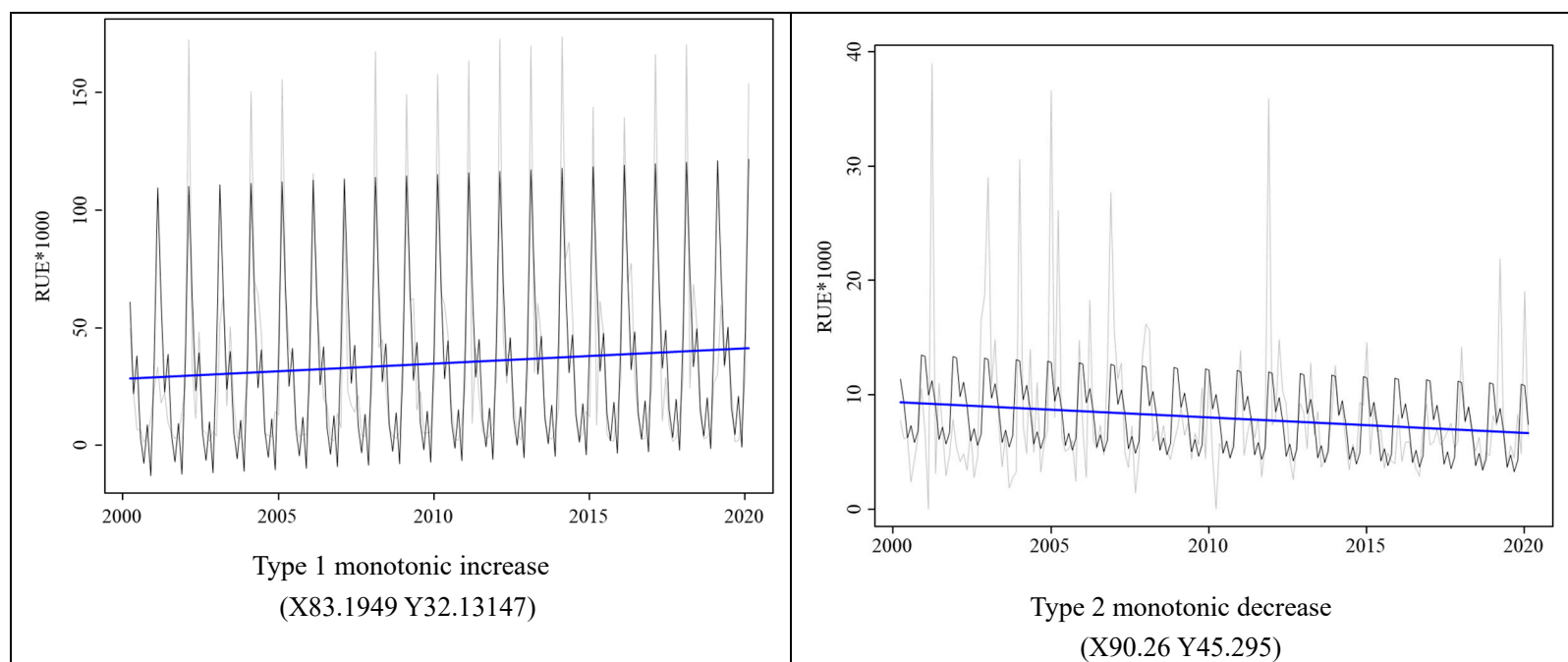


Figure S1. Correlation analysis between the SPEI obtained by AUNSPIN interpolation and the global 0.5 degree SPEI dataset

The results showed that 97.61% of the pixels passed the significance test ($p < 0.05$), mainly distributed in central and eastern Inner Mongolia and most area of the northeastern part. Among them, 37.76% of the pixels were strongly correlated ($r > 0.8$), while 58.74% showed weakly correlations ($0.3 < r < 0.8$). Only 3.5% of the pixels had no correlation, scattering in the northwest, especially in areas where deserts widely distributed. This was most likely due to the scarcity of meteorological stations and the large deviation of the interpolation.



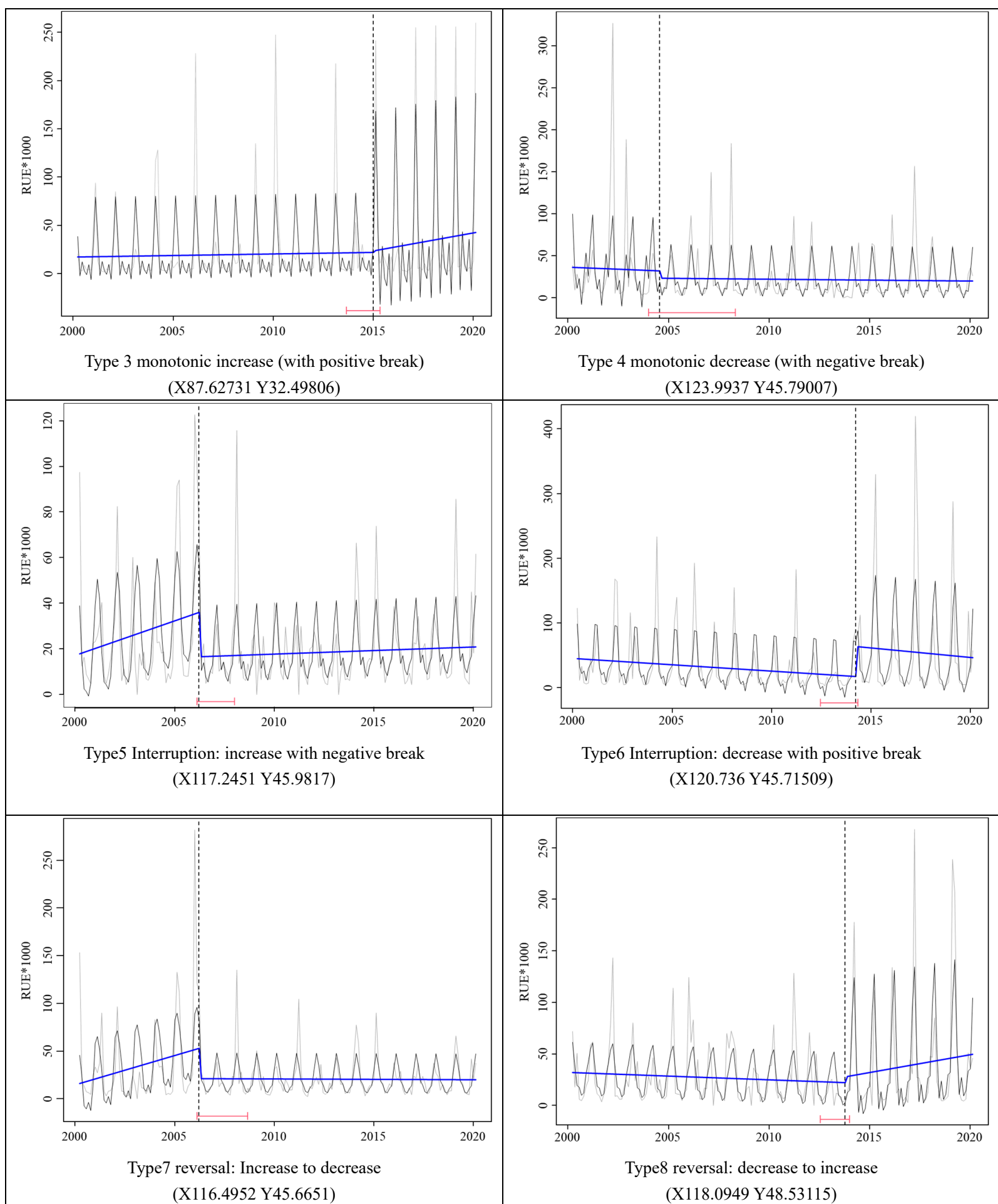


Figure S2. Trend types of ecosystem functioning based on rain use efficiency detected by BFAST01

Table S1 Arguments setting of (a) BFAST01, (b) BFASTclassify, (c) BFAST, and (d) BFASTLite in R 4.1.1(other arguments use default settings)

(a)	
Arguments	Sets
formula	Response~trend+harmon
test	BIC, OLS-MOSUM, supLM,supF
level	0.1
aggregate	any
bandwidth	0.15,
(b)	
Arguments	Sets
alpha	0.1
pct_stable	0.25
typology	"standard"
(c)	
Arguments	Sets
h	0.15
season	harmonic
(d)	
Arguments	Sets
formula	response ~ trend + harmon
order	3
breaks	"BIC"
stl	"both"

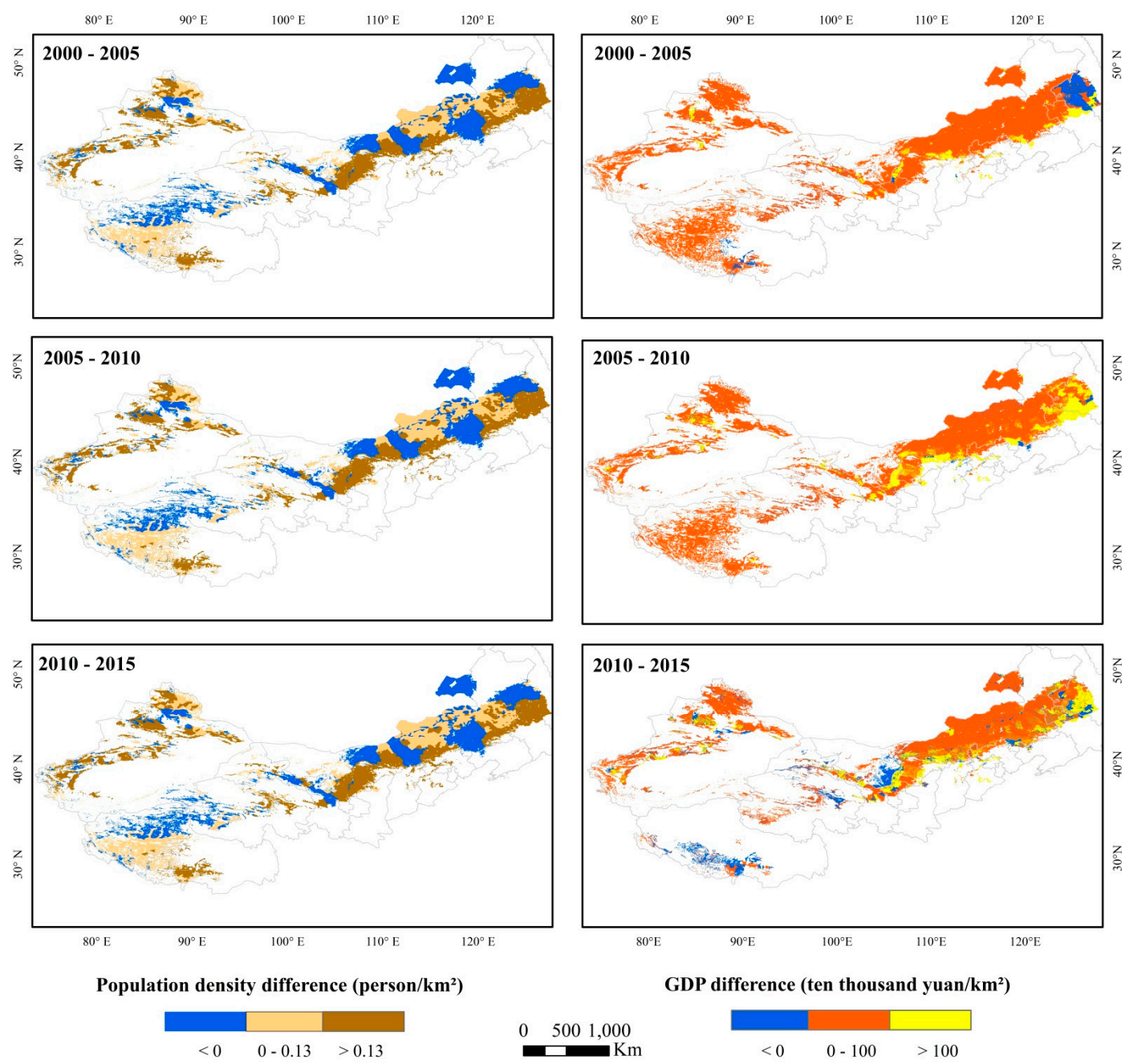


Figure S3. Changes in population density and GDP over a 5-year interval from 2000 to 2015

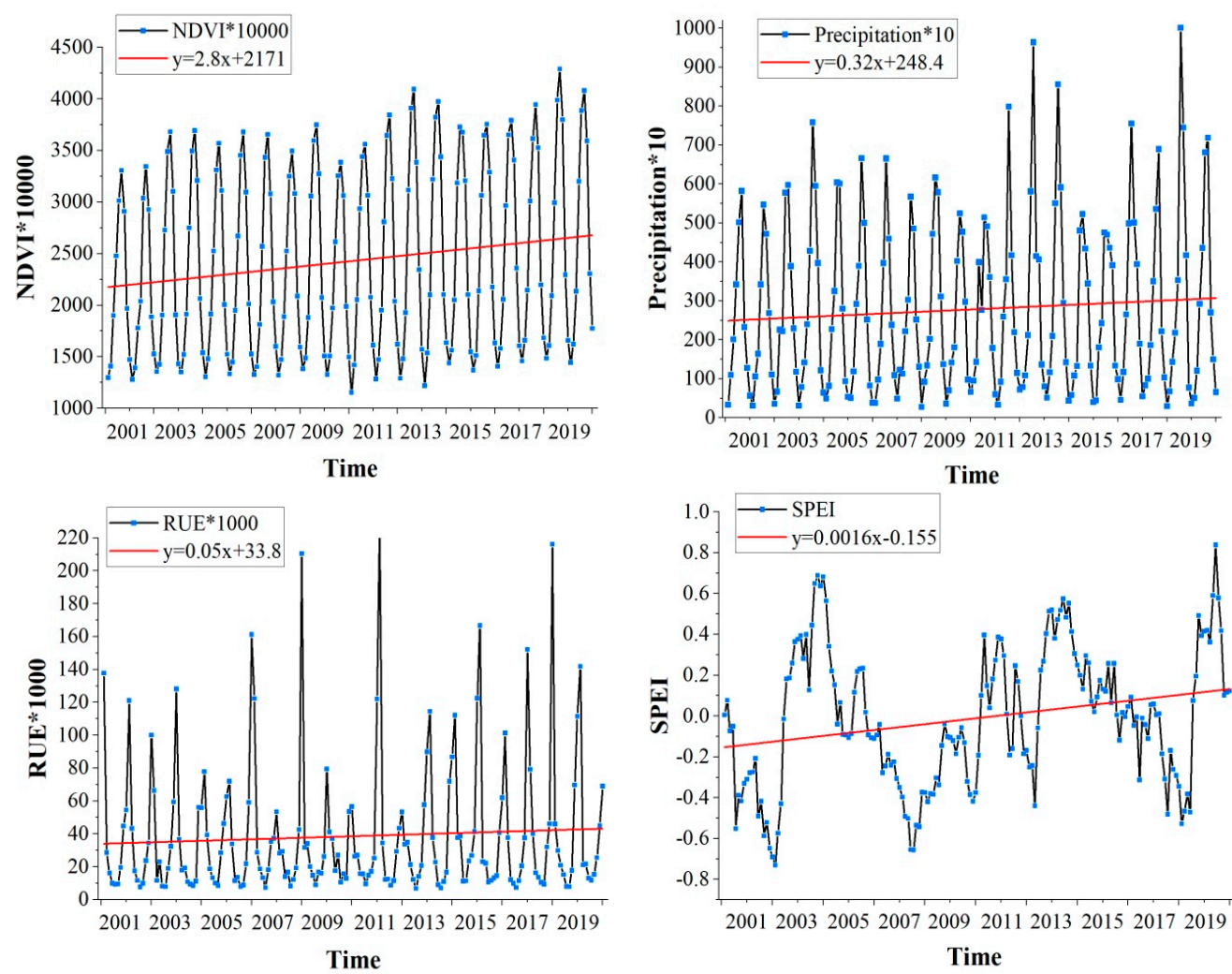


Figure S4. Regional mean NDVI, P, RUE and SPEI from 2000 to 2019 (From March to November every year)

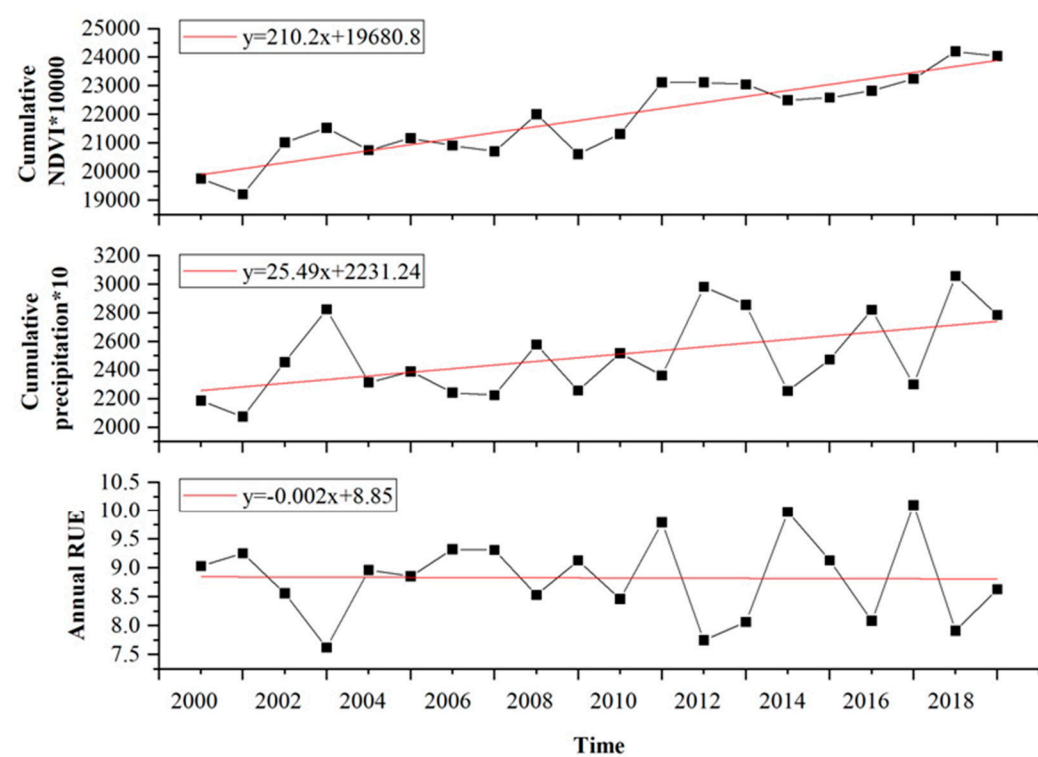
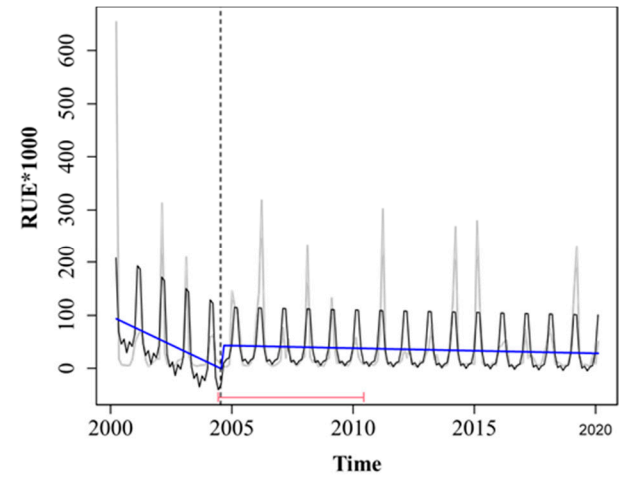
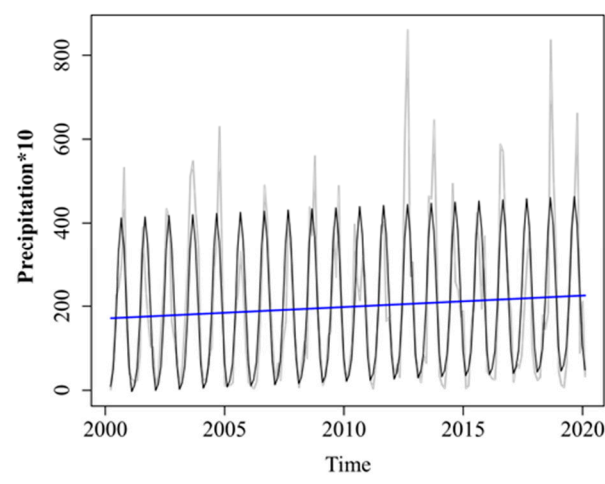
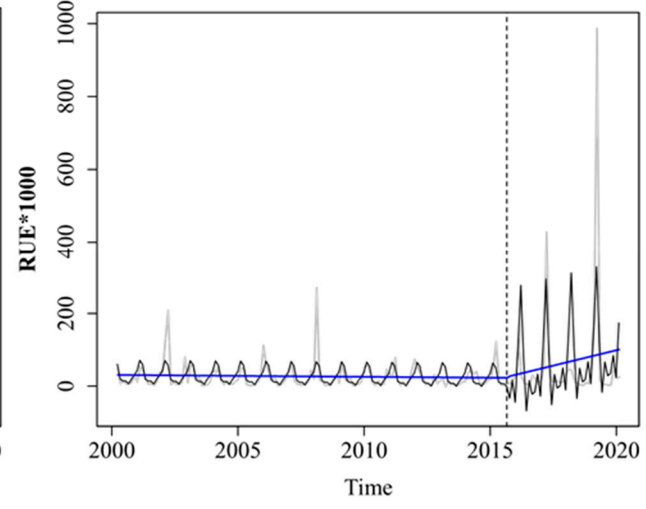
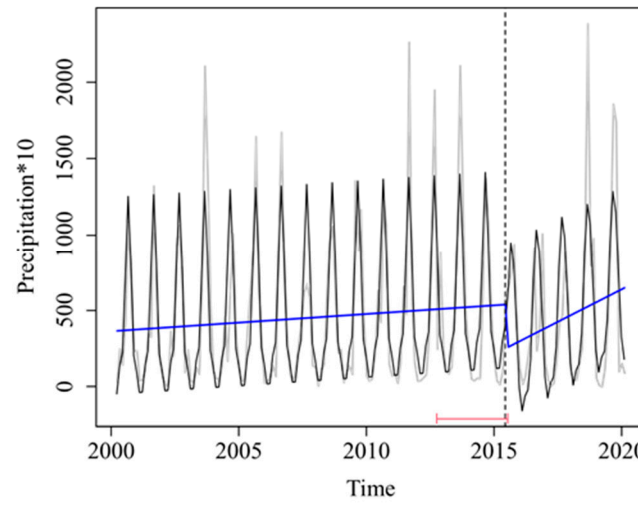


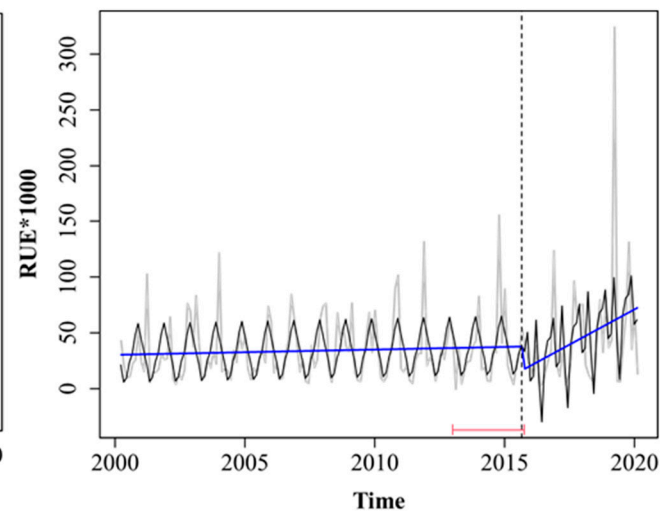
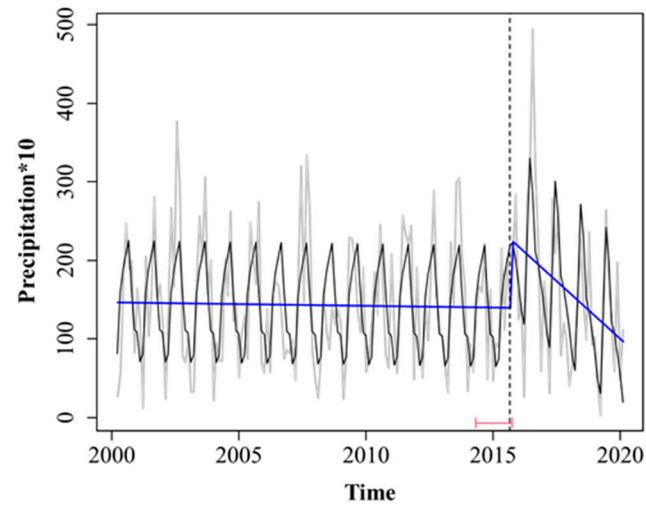
Figure S5. Annual regional mean NDVI, P and RUE from 2000 to 2019 (From March to November every year)
(Annual RUE is obtained by dividing the annual accumulated NDVI by the annual accumulated precipitation)



a. Sample 1: Xilingol League, Central Inner Mongolia (X113.6 Y44.2)



b. Sample 2: Southeast Hulun Buir (X123.3 Y47.8)



c. Sample 3: northern Xinjiang (X 85.54442 Y 44.68714)

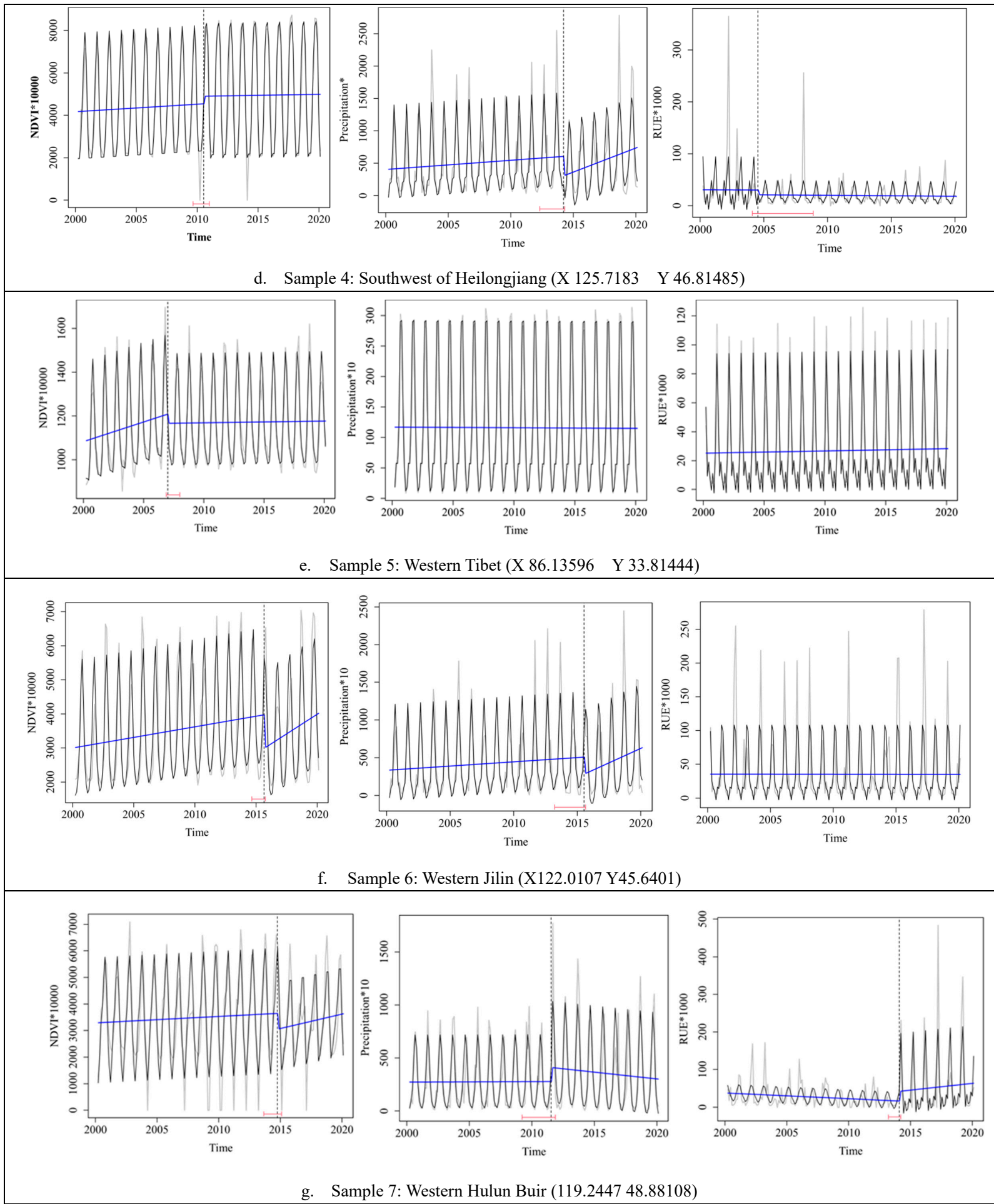


Figure S6: Trend types of some typical samples detected by BFAST01 model

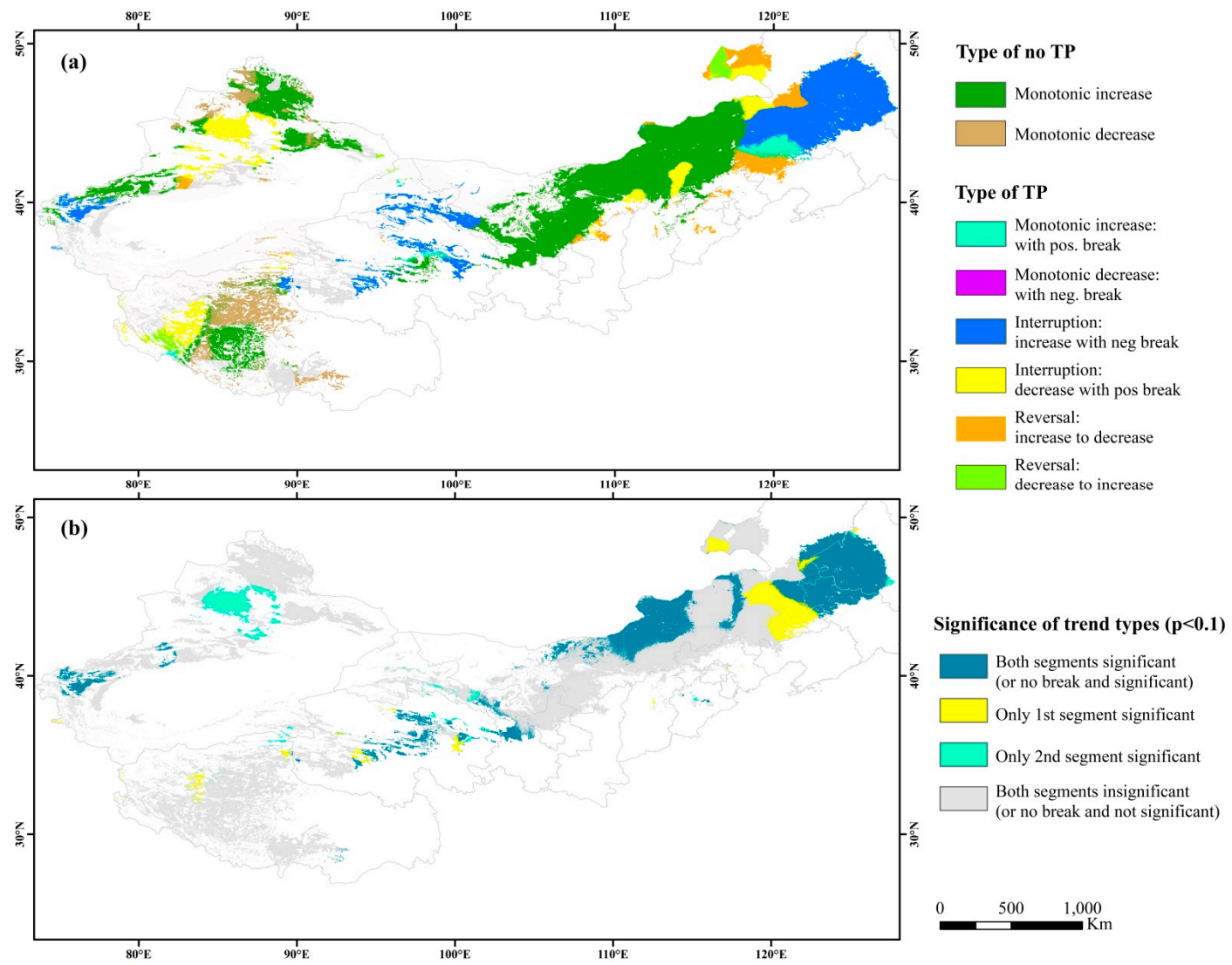


Figure S7. Distribution of break types of precipitation (a) and significance test of break types (b) ($p < 0.1$)

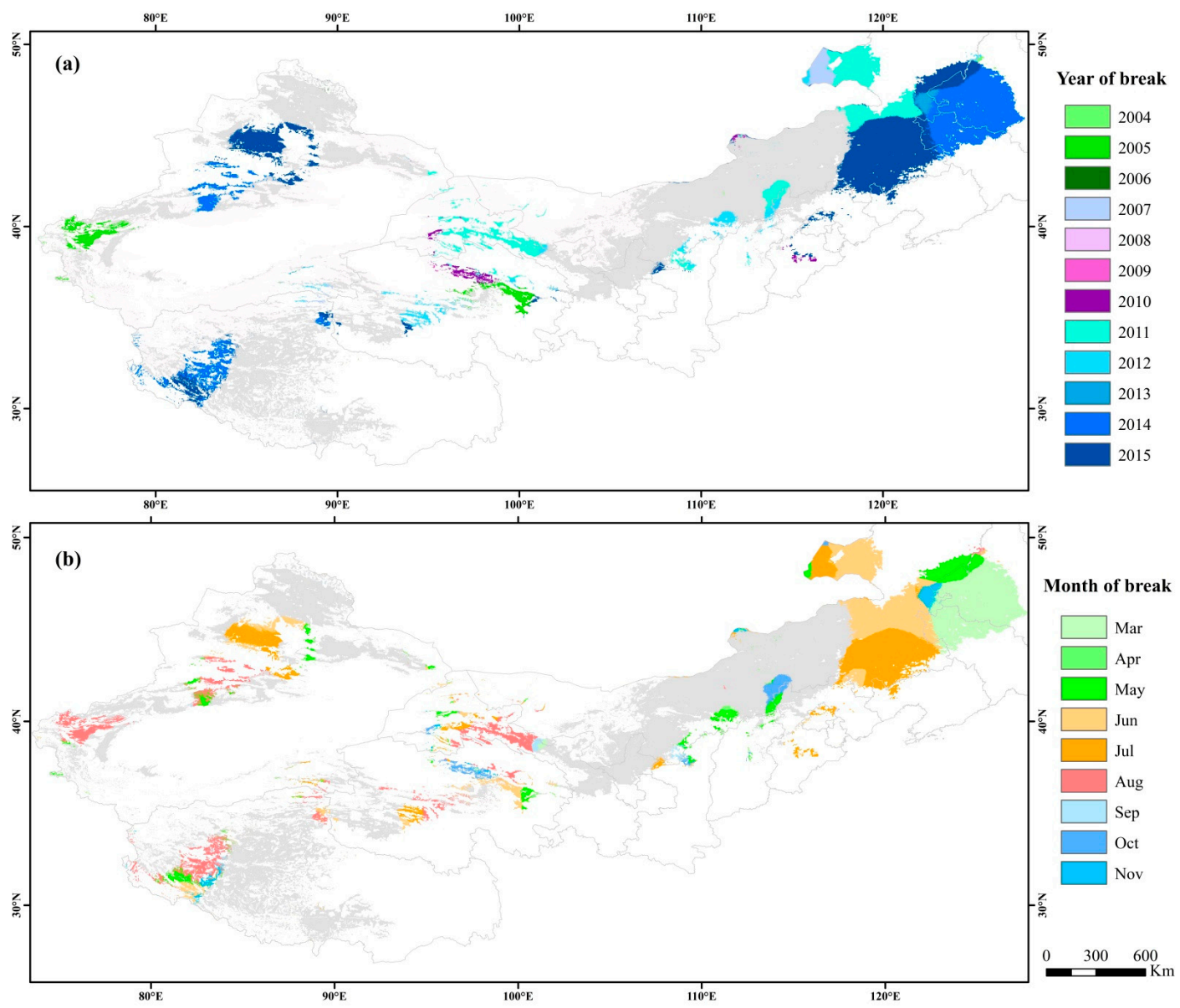


Figure S8. Timing of TPs in precipitation ($p < 0.1$): (a) year; (b) month.

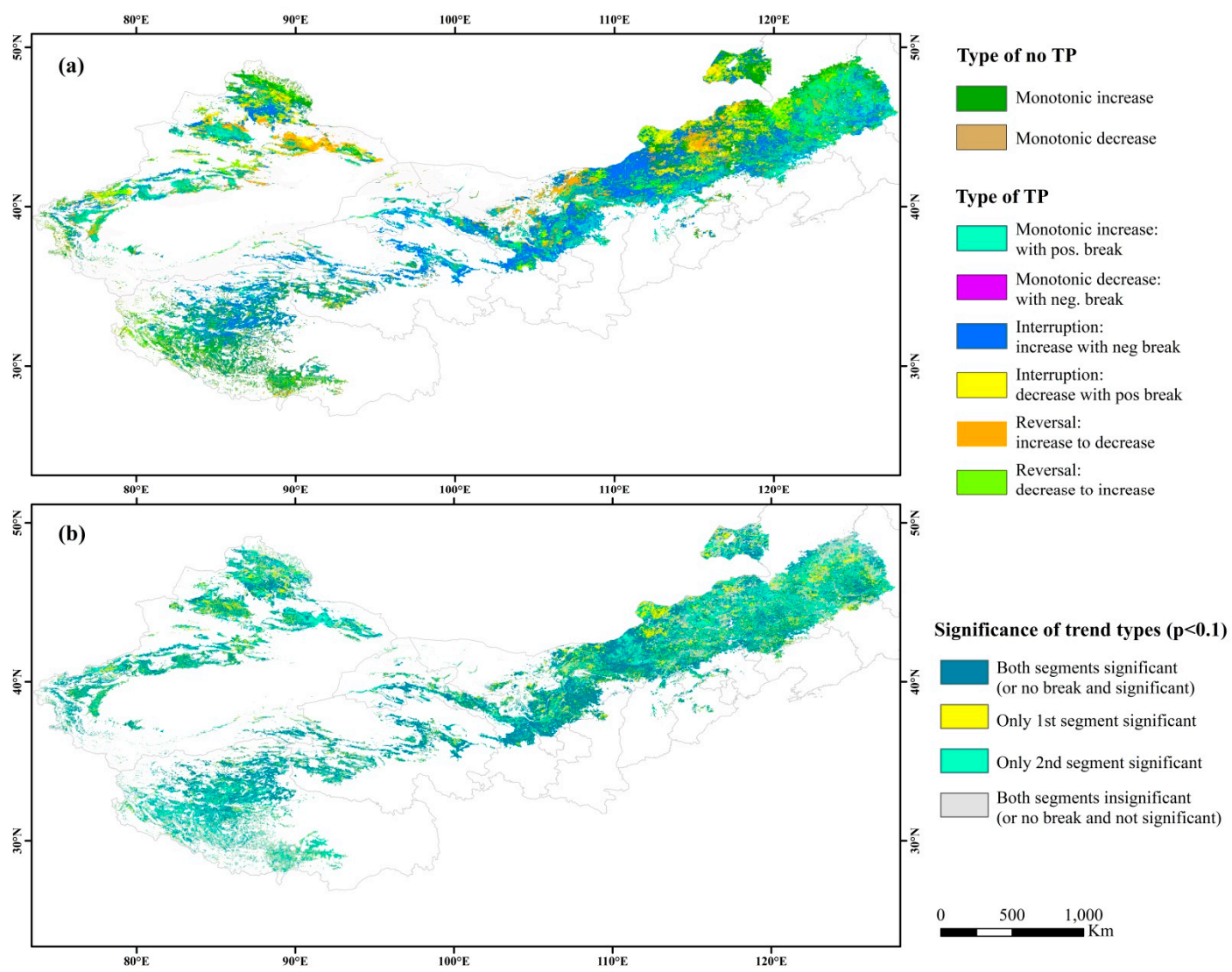


Figure S9. Distribution of break types of NDVI (a) and significance test of break types (b) ($p < 0.1$)

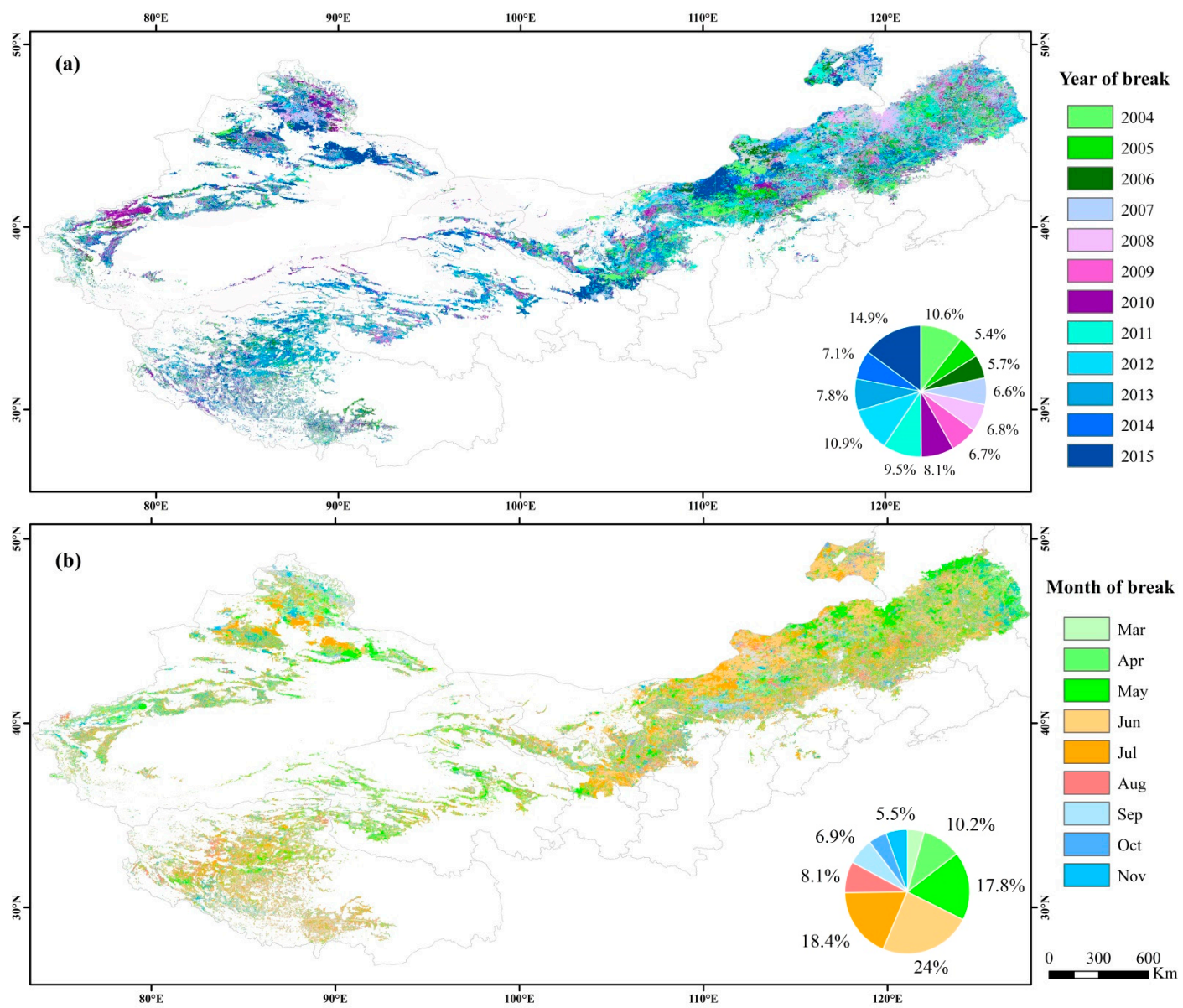


Figure S10. Timing of TPs in NDVI ($p < 0.1$): (a) year; (b) month.

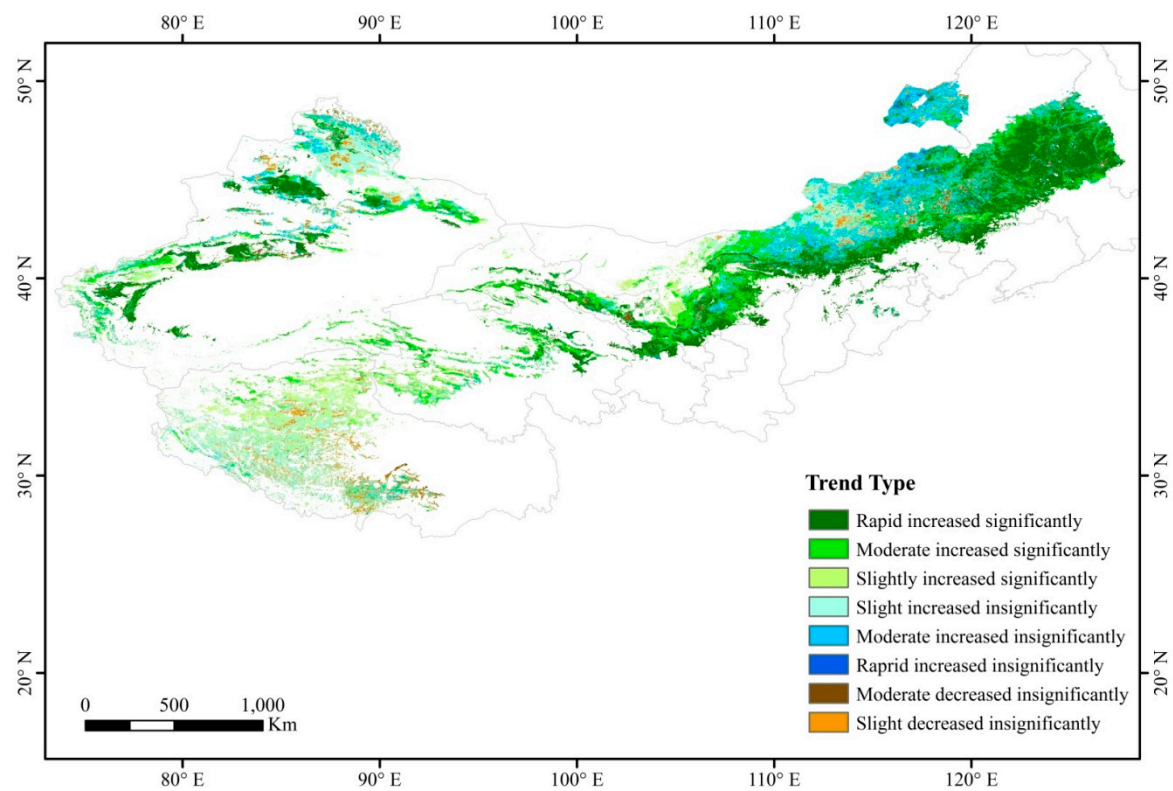


Figure S11. Inter-annual variation Sen trend of annual cumulative (March-November) NDVI

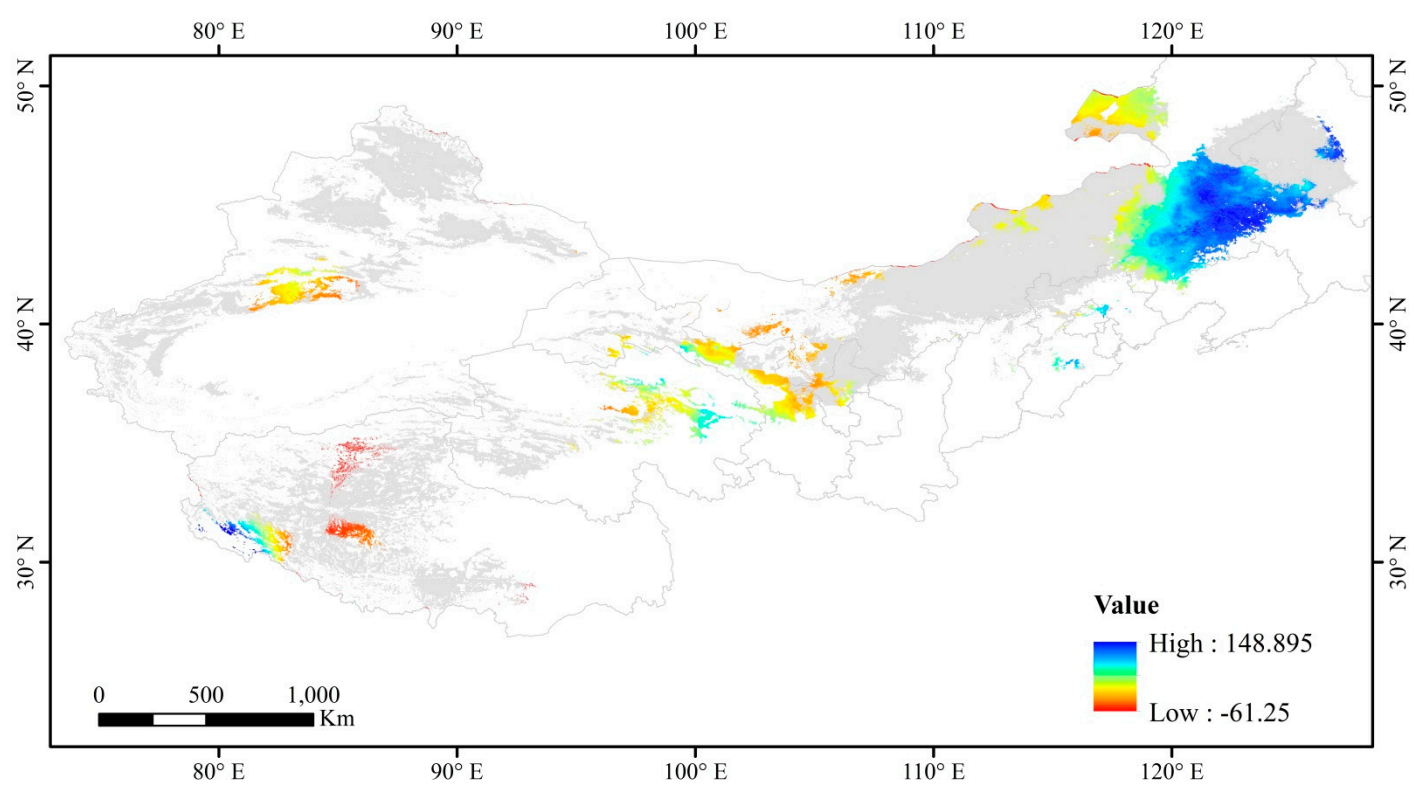


Figure S12. Inter-annual variation Sen trend of annual cumulative (March-November) precipitation

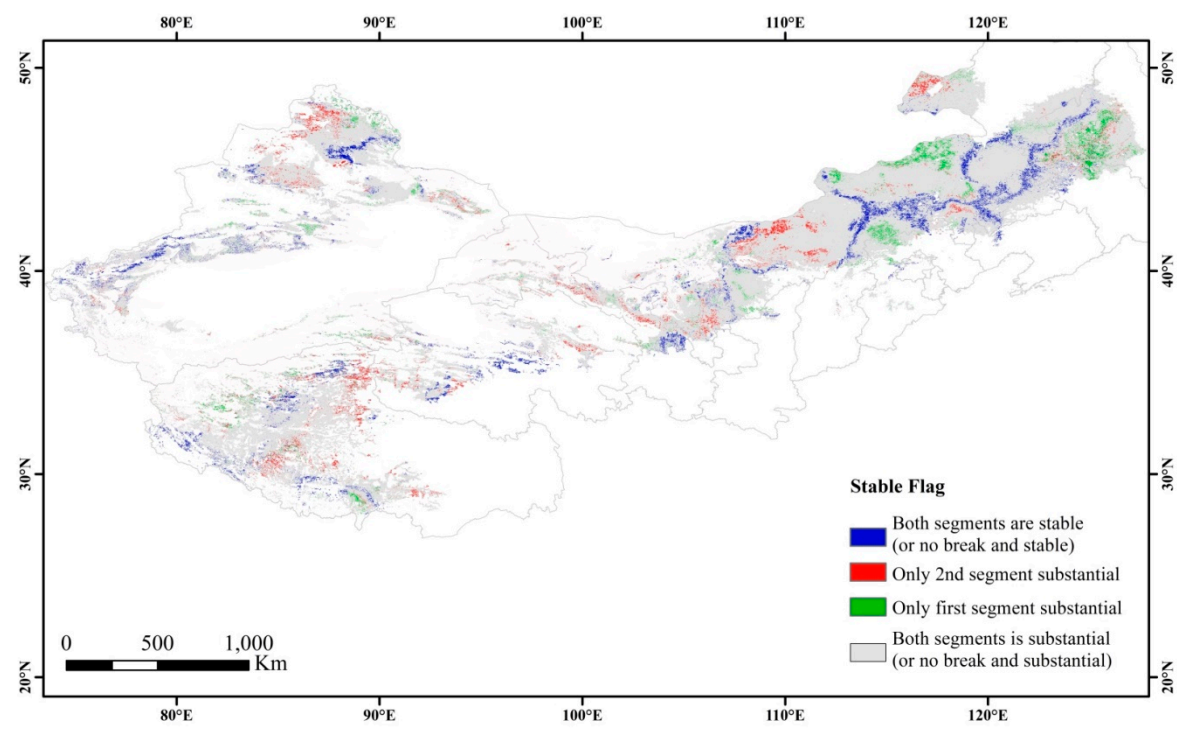


Figure S13. Spatial distribution of stable ecosystem function change

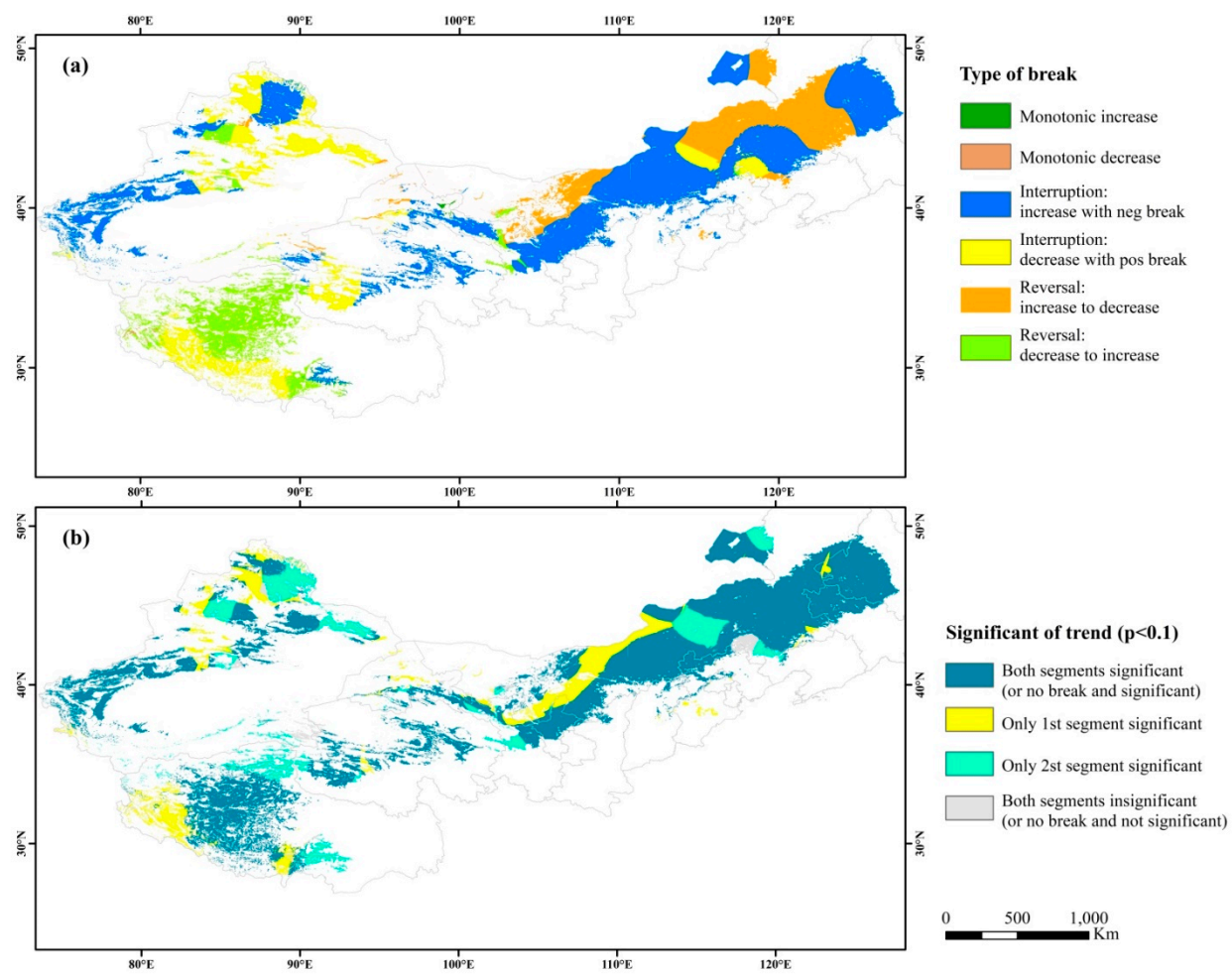
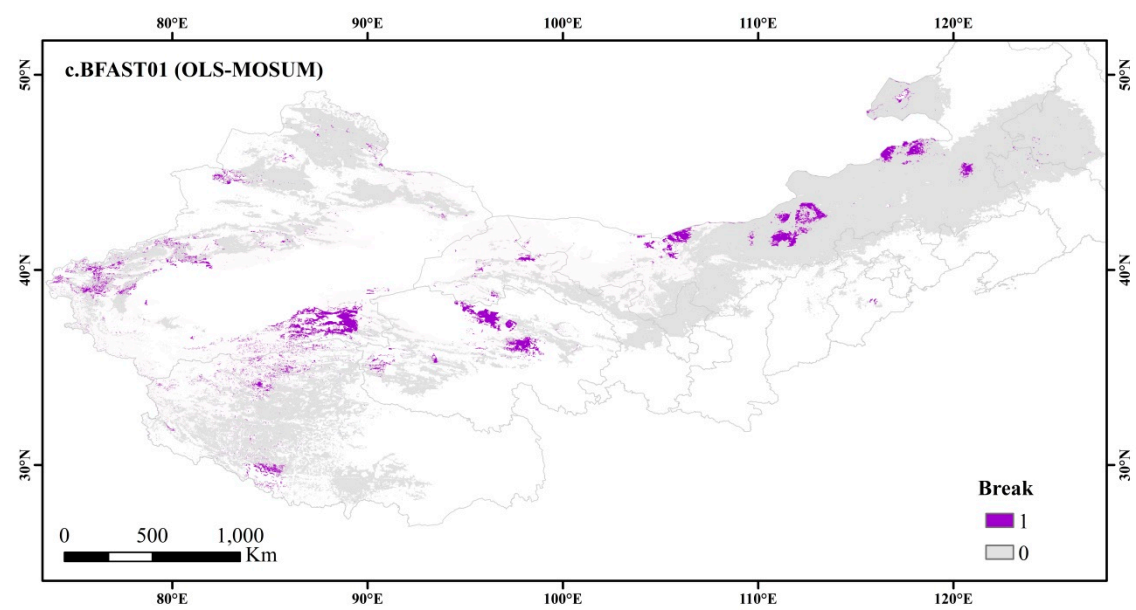
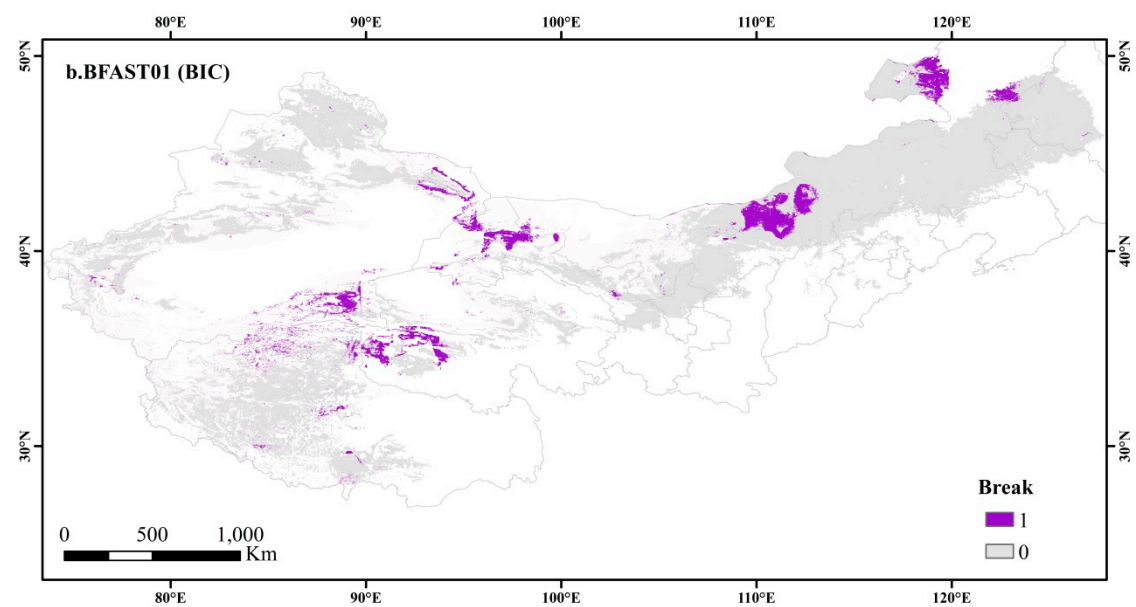
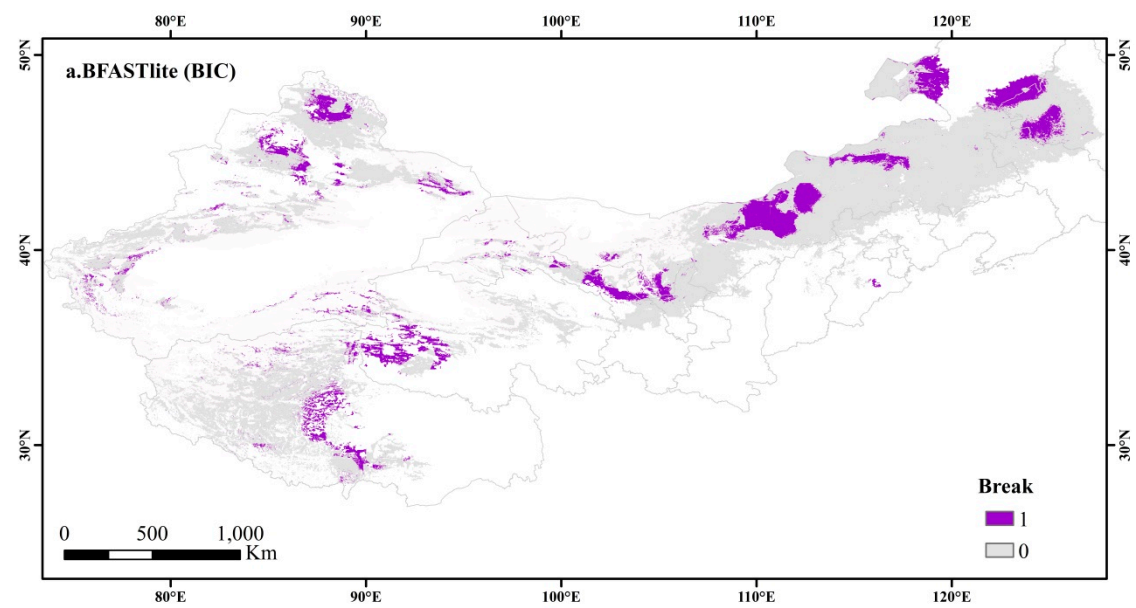


Figure S14. Distribution of break types of SPEI (a) and significance test of break types (b) ($p < 0.1$)



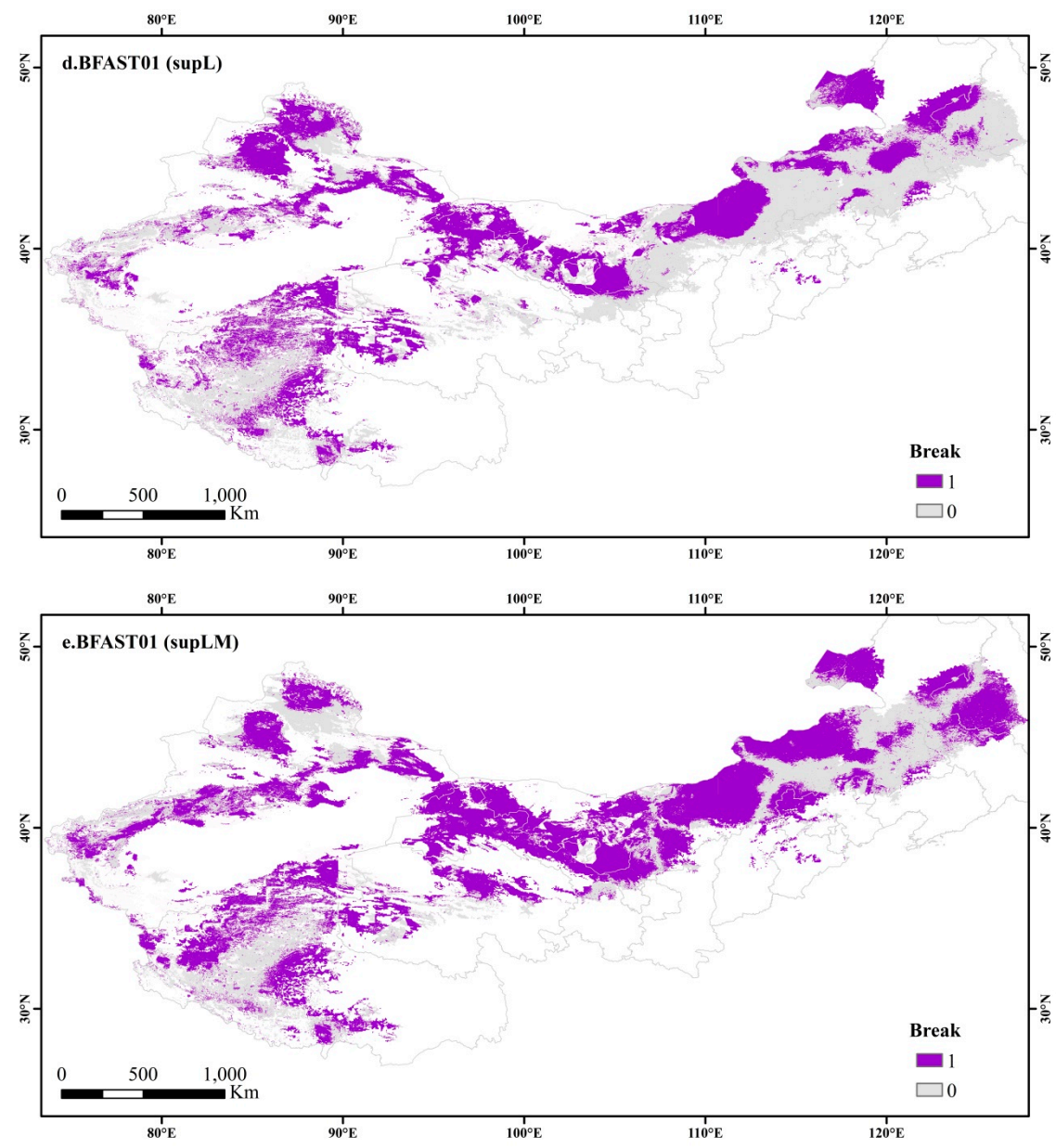


Figure S15. The spatial distribution map of TPs obtained by BFASTlite and the four test methods of BFAST01 (all the above results have been tested for significance $p < 0.1$), from top to bottom: a.BFASTlite_BIC b.BFAST01_BIC c.BFAST01_OLS-MOSUM d.BFAST01_supL e.BFAST01_supLM